

Communication

Potential α -Glucosidase Inhibitors from the Deep-Sea Sediment-Derived Fungus *Aspergillus insulicola*

Weibo Zhao ^{1,2,†}, Yanbo Zeng ^{2,3,†} , Wenjun Chang ^{2,3}, Huiqin Chen ², Hao Wang ² , Haofu Dai ² and Fang Lv ^{1,*}

¹ Beijing Key Laboratory for Separation and Analysis in Biomedicine and Pharmaceuticals, School of Life Science, Beijing Institute of Technology, Beijing 100081, China

² Hainan Provincial Key Laboratory for Functional Components Research and Utilization of Marine Bio-Resources, Institute of Tropical Bioscience and Biotechnology, Chinese Academy of Tropical Agricultural Sciences & Key Laboratory for Biology and Genetic Resources of Tropical Crops of Hainan Province, Hainan Institute for Tropical Agricultural Resources, Haikou 571101, China

³ Zhanjiang Experimental Station of Chinese Academy of Tropical Agricultural Sciences, Zhanjiang 524013, China

* Correspondence: lvfangbeijing@bit.edu.cn

† These authors contributed equally to this work.

Abstract: Three new phenolic compounds, epicoconigrone C–D (1–2) and flavimycin C (3), together with six known phenolic compounds: epicoconigrone A (4); 2-(10-formyl-11,13-dihydroxy-12-methoxy-14-methyl)-6,7-dihydroxy-5-methyl-4-benzofurancarboxaldehyde (5); epicoconide B (6); eleganketal A (7); 1,3-dihydro-5-methoxy-7-methylisobenzofuran (8); and 2,3,4-trihydroxy-6-(hydroxymethyl)-5-methylbenzyl-alcohol (9), were isolated from fermentation cultures of a deep-sea sediment-derived fungus, *Aspergillus insulicola*. Their planar structures were elucidated based on the 1D and 2D NMR spectra and HRESIMS data. The absolute configurations of compounds 1–3 were determined by ECD calculations. Compound 3 represented a rare fully symmetrical isobenzofuran dimer. All compounds were evaluated for their α -glucosidase inhibitory activity, and compounds 1, 4–7, and 9 exhibited more potent α -glucosidase inhibitory effect with IC₅₀ values ranging from 17.04 to 292.47 μ M than positive control acarbose with IC₅₀ value of 822.97 μ M, indicating that these phenolic compounds could be promising lead compounds of new hypoglycemic drugs.

Keywords: marine fungus; *Aspergillus insulicola*; phenolic compounds; ECD calculations; α -glucosidase inhibition



Citation: Zhao, W.; Zeng, Y.; Chang, W.; Chen, H.; Wang, H.; Dai, H.; Lv, F. Potential α -Glucosidase Inhibitors from the Deep-Sea Sediment-Derived Fungus *Aspergillus insulicola*. *Mar. Drugs* **2023**, *21*, 157. <https://doi.org/10.3390/md21030157>

Academic Editor: Emiliano Manzo

Received: 4 February 2023

Revised: 23 February 2023

Accepted: 24 February 2023

Published: 26 February 2023



Copyright: © 2023 by the authors. Licensee MDPI, Basel, Switzerland. This article is an open access article distributed under the terms and conditions of the Creative Commons Attribution (CC BY) license (<https://creativecommons.org/licenses/by/4.0/>).

1. Introduction

According to the International Diabetes Federation, 537 million people worldwide were diagnosed with diabetes mellitus in 2021, and about 90 percent of them were type 2 diabetes mellitus (T2DM) [1,2]. T2DM is a chronic metabolic disease that is characterized by postprandial hyperglycemia in the case of insulin resistance and relative lack of insulin [3]. The inhibition of α -glucosidase can reduce the cleavage of glucose from disaccharides or oligosaccharides to inhibit postprandial hyperglycemia [4]. Therefore, α -glucosidase is a common therapeutic target for the treatment of T2DM [5]. Currently available α -glucosidase inhibitors, such as acarbose, voglibose and miglitol, have been used to treat T2DM patients. Nevertheless, the use of these drugs has been associated with serious side effects, such as abdominal distension and diarrhea [6,7]. For this reason, the search for natural, efficient and non-toxic α -glucosidase inhibitors provides an attractive strategy for the development of new hypoglycemic drugs.

Phenolic compounds have been proved to be effective α -glucosidase inhibitors [8–11]. Marine phenolic compounds are far less researched than those from terrestrial sources, which could suggest great potential in the ocean to develop novel diabetes drugs [12]. Some marine phenolic compounds isolated from seaweed [13,14] and seagrass [15] have been

confirmed to have wonderful α -glucosidase inhibitory activity. In order to find more marine phenolic compounds with α -glucosidase inhibitory activity, our team studied marine fungi from the South China Sea. *Aspergillus insulicola*, a fungi previously not extensively studied, had great development and utilization value. Previous chemical studies of *A. insulicola* have discovered many peptides [16–18] and nitrobenzoyl sesquiterpenoids [19,20], which showed significant biological activities, including anti-bacteria [16] and cytotoxic [19,20]. During our ongoing research in finding new compounds with potential bioactivities [21–23], a chemical investigation of the deep-sea sediment-derived fungus *A. insulicola* led to the isolation and identification of three new phenolic compounds, epicocconigrone C–D (1–2) and flavimycin C (3), together with six known phenolic compounds (4–9) (Figure 1). All compounds were investigated for their α -glucosidase inhibitory activity. Herein, we describe the structure elucidation of the new metabolites as well as the α -glucosidase inhibitory activity of the isolated compounds.

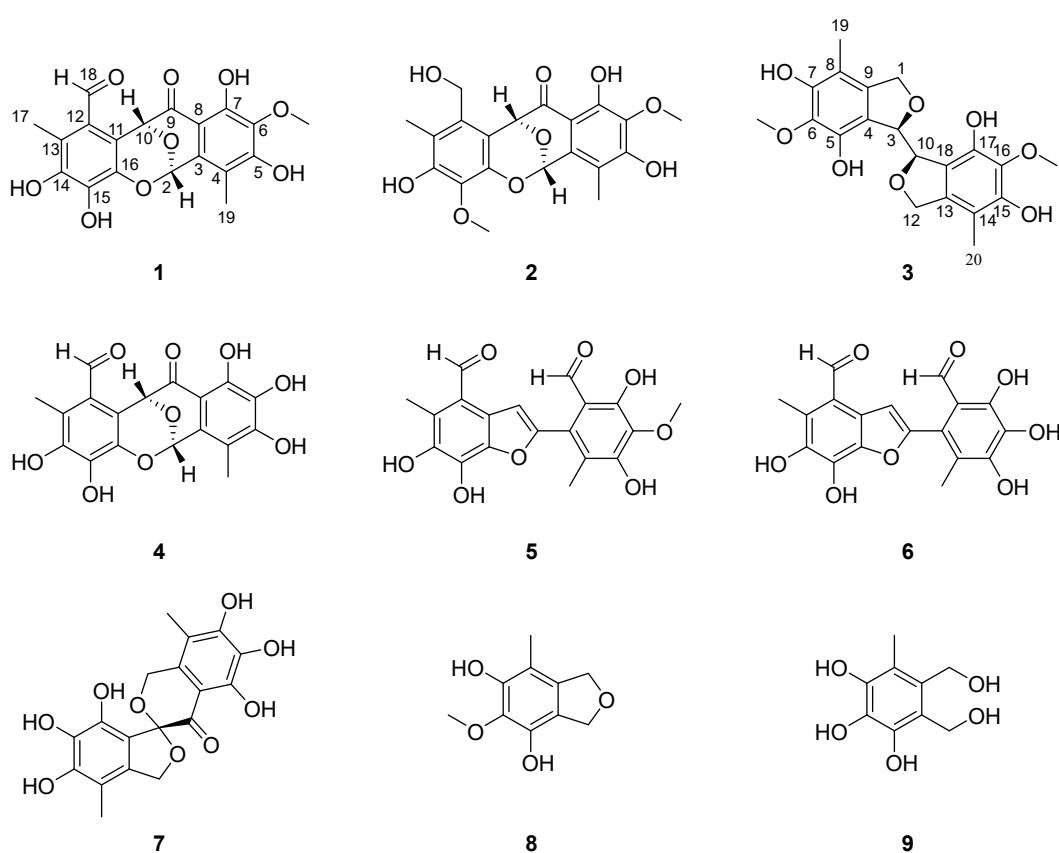


Figure 1. Structures of compounds 1–9 from *Aspergillus insulicola*: epicocconigrone C–D (1–2); flavimycin C (3); epicocconigrone A (4); 2-(10-formyl-11,13-dihydroxy-12-methoxy-14-methyl)-6,7-dihydroxy-5-methyl-4-benzofurancarboxaldehyde (5); epicoccolide B (6); eleganketal A (7); 1,3-dihydro-5-methoxy-7-methylisobenzofuran (8); and 2,3,4-trihydroxy-6-(hydroxymethyl)-5-methylbenzyl-alcohol (9).

2. Results and Discussion

2.1. Structure Elucidation of New Compounds 1–3

Epicocconigrone C (1) was isolated as a yellow solid, and its molecular formula was determined to be $C_{19}H_{16}O_9$ with 12 degrees of unsaturation by HRESIMS data at m/z 411.0698 (calcd. 411.0687 for $C_{19}H_{16}O_9Na$, $[M + Na]^+$), which was supported by the ^{13}C NMR and DEPT spectral data. The IR spectrum of 1 featured typical absorption bands for hydroxyl (3413 cm^{-1}) and conjugated ketone (1670 cm^{-1}). The 1H NMR spectrum (Table 1) of 1 revealed two methyls (δ_H 2.26 and δ_H 2.31), one methoxy (δ_H 3.70), two oxymethines (δ_H 6.38 and δ_H 6.83), one aldehyde proton (δ_H 10.34), and one hydroxyl

proton (δ_{H} 11.33). The ^{13}C NMR (Table 2) and DEPT spectra showed 19 well-resolved carbon atom signals, including one ketone carbonyl (δ_{C} 196.9), one aldehydic carbonyl (δ_{C} 191.2), two oxygenated tertiary carbons (δ_{C} 89.8 and δ_{C} 68.6), one methoxy carbon (δ_{C} 60.2), two methyls (δ_{C} 11.8 and δ_{C} 10.2), and twelve olefinic quaternary carbons at δ_{C} 156.9–104.5, accounting for 8 degrees of unsaturation. Thus, compound **1** was thought to possess a tetracyclic skeleton. The strong heteronuclear multiple-bond correlation (HMBC) correlations from H-17 (δ_{H} 2.31) to C-12 (δ_{C} 121.7), C-13 (δ_{C} 121.9), and C-14 (δ_{C} 144.3), from H-18 (δ_{H} 10.34) to C-11 (δ_{C} 112.6), C-12, C-13, and C-14, as well as the weak signals from H-17 to C-11, C-15 (δ_{C} 138.4), and C-16 (δ_{C} 135.8) confirmed the existence of ring A (Figure 2). The HMBC correlations from H-19 (δ_{H} 2.26) to C-3 (δ_{C} 130.8), C-4 (δ_{C} 115.8), and C-5 (δ_{C} 156.9), as well as the HMBC correlations from 7-OH (δ_{H} 11.33) to C-6, C-7 (δ_{C} 153.6), and C-8 (δ_{C} 104.5) established the substitution of the aromatic ring D. Furthermore, the HMBC correlations from H-2 (δ_{H} 6.83) to C-10 (δ_{C} 68.6) and C-16, from H-10 (δ_{H} 6.38) to C-2 (δ_{C} 89.8), C-11, C-12 and C-16 suggested the presence of two oxygen bridges between C-16/C-2 and C-2/C-10 in ring B, which could be confirmed by the low field chemical shift signal of CH-2 (δ_{C} 89.8, δ_{H} 6.83). Ring C was established by the HMBC correlations from H-2 to C-4 and C-8, and from H-10 to C-8 and C-9 (δ_{C} 196.9). The comprehensive NMR analysis indicated that **1** shared the same oxygen-bridged skeleton with epicocconigrone A (**4**) [24], with the exception that the appearance of 6-OCH₃ in **1** replaced 6-OH in **4**, which was supported by the HMBC correlation from 6-OCH₃ (δ_{H} 3.70) to C-6 (δ_{C} 134.7). Thus, the planar structure of **1** was elucidated as shown (Figure 1), named epicocconigrone C. In the nuclear Overhauser effect spectroscopy (NOESY) spectrum of **1**, the correlation between H-2 and H-10 was indicative of their *cis* relationship (Figure 2). The absolute configuration of **1** was confirmed by the ECD calculation. Its experimental ECD curve for the absolute configurations of 2*S* and 10*R* was consistent with the calculated ECD curve of (2*S*, 10*R*) (Figure 3).

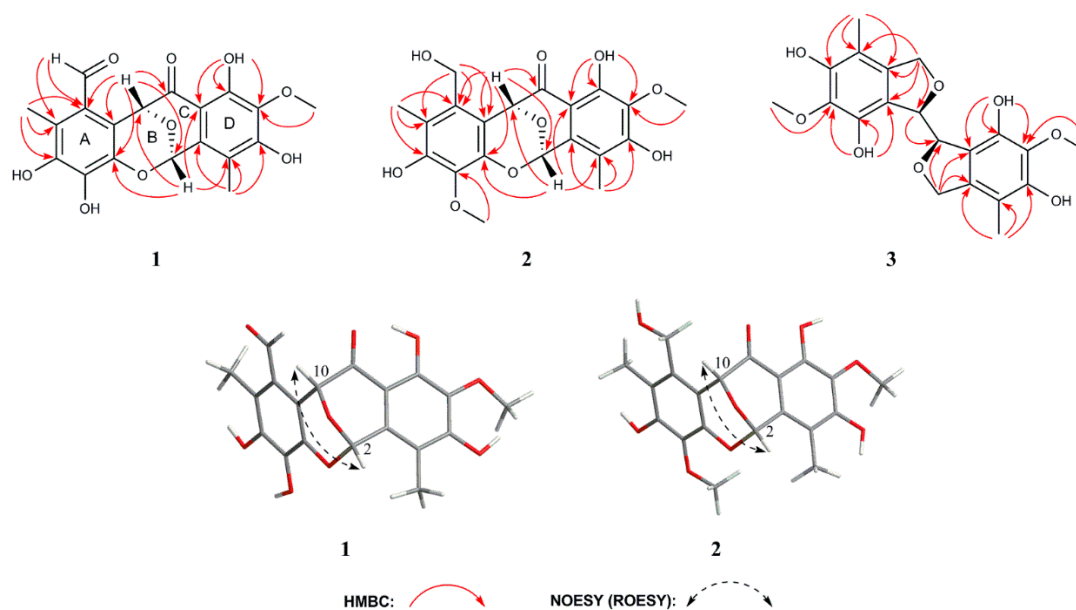
Table 1. ^1H NMR data of epicocconigrone C–D (**1**–**2**) and flavimycin C (**3**) (δ in ppm, *J* in Hz) in DMSO-*d*₆.

Position	1 ^a	2 ^a	3 ^b
1			4.54 (d, 15.0) 4.65 (d, 15.0)
2	6.83, s	6.76, s	
3			4.30, s
10	6.38, s	5.65, s	4.30, s
12			4.54 (d, 15.0) 4.65 (d, 15.0)
17	2.31, s	2.09, s	
18	10.34, s	4.81 (d, 12.1) 4.32 (d, 12.1)	
19	2.26, s	2.18, s	1.88, s
20			1.88, s
6-OCH ₃	3.70, s	3.57, s	3.64, s
14-OCH ₃			3.64, s
15-OCH ₃		3.69, s	
5-OH			8.55, s
7-OH	11.33, s	11.46, s	8.68, s
14-OH		8.92, s	
15-OH			8.68, s
17-OH			8.55, s

^a Recorded at 500 MHz; ^b Recorded at 600 MHz.

Table 2. ^{13}C NMR (125 MHz) data of epicocconigrone C-D (1–2) and flavimycin C (3) in $\text{DMSO-}d_6$.

Position	1	2	3
1			65.8, CH ₂
2	89.8, CH	89.9, CH	
3	130.8, C	131.0, C	66.1, CH
4	115.8, C	115.8, C	112.2, C
5	156.9, C	158.9, C	147.0, C
6	134.7, C	134.6, C	134.3, C
7	153.6, C	153.6, C	147.8, C
8	104.5, C	103.4, C	109.7, C
9	196.9, C	196.8, C	129.7, C
10	68.6, CH	70.3, CH	66.1, CH
11	112.6, C	108.3, C	
12	121.7, C	132.1, C	65.8, CH ₂
13	121.9, C	118.1, C	129.7, C
14	144.3, C	148.5, C	109.7, C
15	138.4, C	134.6, C	147.8, C
16	135.8, C	140.3, C	134.3, C
17	11.8, CH ₃	11.0, CH ₃	147.0, C
18	191.2, CH	55.8, CH ₂	112.2, C
19	10.2, CH ₃	10.3, CH ₃	9.5, CH ₃
20			9.5, CH ₃
6-OCH ₃	60.2, CH ₃	60.3, CH ₃	60.2, CH ₃
14-OCH ₃			60.2, CH ₃
15-OCH ₃		60.0, CH ₃	

**Figure 2.** Key HMBC correlations of compounds 1–3 and key NOESY/ROESY correlations of compounds 1–2.

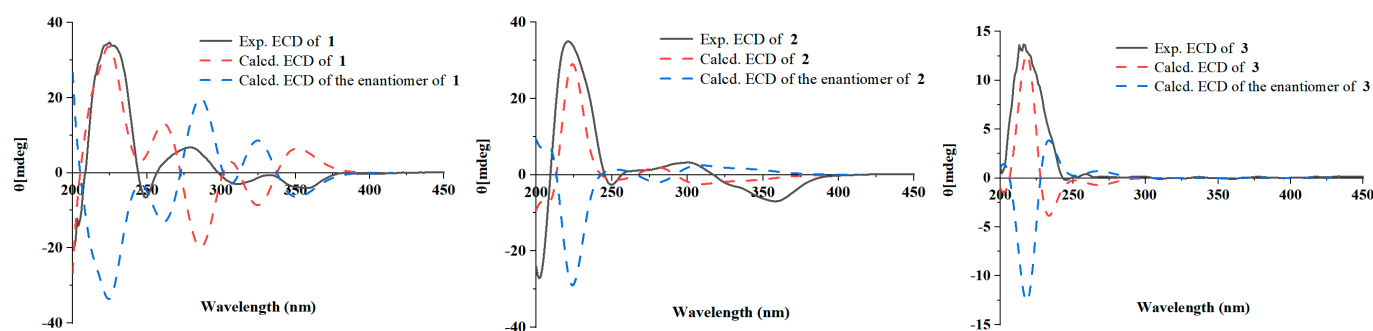


Figure 3. Experimental and calculated ECD spectra of compounds 1–3.

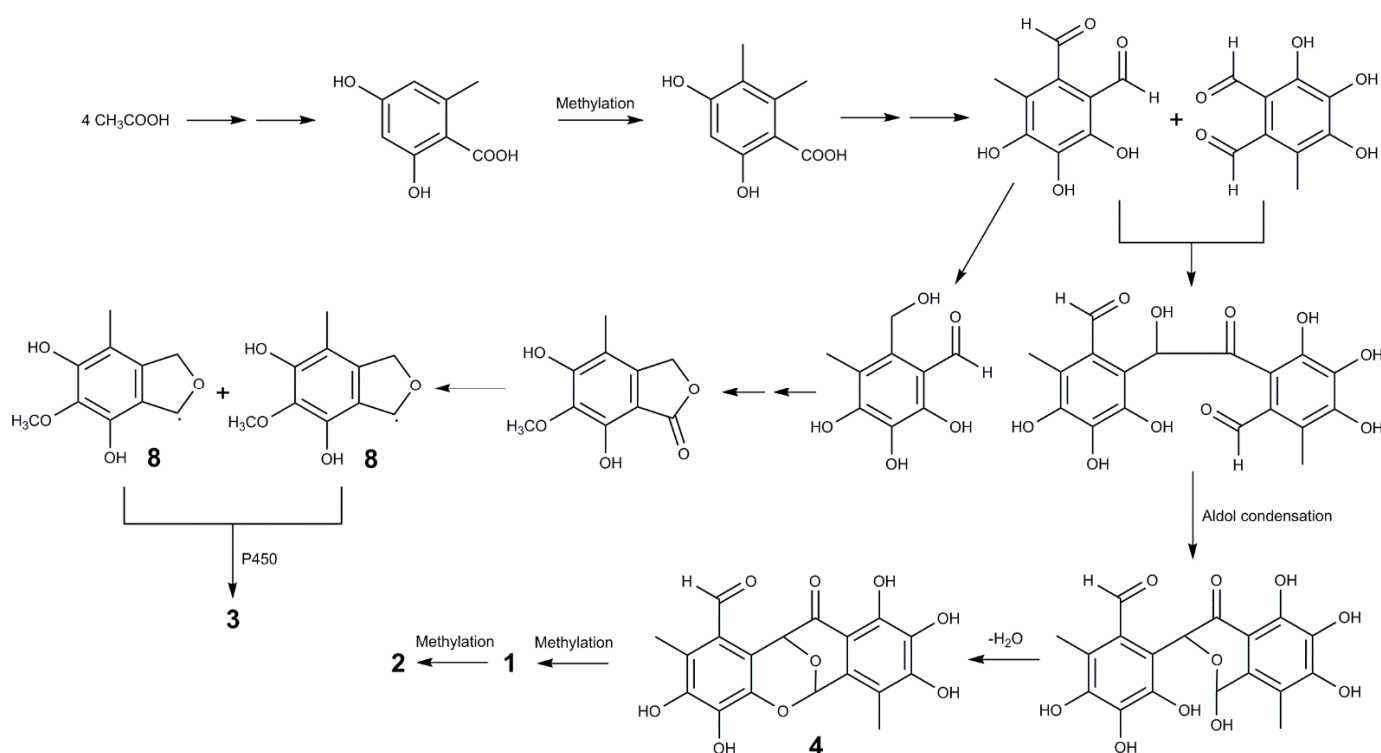
Epicocconigrone D (**2**) was obtained as a yellow solid. The molecular formula of **2** was determined as $C_{20}H_{20}O_9$ with 11 unsaturated degrees by HRESIMS data at m/z 427.1004 (calcd. 427.1000 for $C_{20}H_{20}O_9Na$, $[M + Na]^+$), which was supported by the ^{13}C NMR and DEPT spectral data. The IR spectrum of **2** featured typical absorption bands for hydroxyl (3446 cm^{-1}) and conjugated ketone (1626 cm^{-1}). The 1H NMR spectrum (Table 1) of **2** indicated two methyl groups (δ_H 2.09 and δ_H 2.18), two methoxy groups (δ_H 3.57 and δ_H 3.69), one methylene (δ_H 4.32, d, $J = 12.1\text{ Hz}$; 4.81 d, $J = 12.1\text{ Hz}$), two oxymethines (δ_H 5.65 and δ_H 6.76), and two hydroxyl protons (δ_H 8.92 and δ_H 11.46). The ^{13}C NMR (Table 2) and DEPT spectra revealed 20 carbon atom signals, including one ketone carbonyl (δ_C 196.8), two oxygenated tertiary carbons (δ_C 89.9 and δ_C 70.3), two methoxy carbons (δ_C 60.3 and δ_C 60.0), one methylene (δ_C 55.8), two methyls (δ_C 11.0 and δ_C 10.3), and twelve olefinic quaternary carbons. Detailed analysis of 2D NMR spectra of **2** revealed that it had a similar structure to **1**. The major differences in **2** were a hydroxymethylene group and a methoxy group substituted at C-12 and C-15, instead of the aldehyde group and the hydroxyl group, respectively, when compared to **1** (Figure 2), which were further confirmed by the HMBC correlations from H₂-18 (δ_H 4.32, 4.81) to C-11 (δ_C 108.3), C-12 (δ_C 132.1), and C-13 (δ_C 118.1), and from 15-OCH₃ (δ_H 3.69) to C-15 (δ_C 134.6). Thus, the planar structure of **2** was elucidated as shown (Figure 1), named epicocconigrone D. The ROESY correlation between H-2 and H-10 indicated their *cis* orientation (Figure 2). The absolute configuration of **2** was understood to be 2*S*, 10*R* by comparing the experimental and simulated ECD curves (Figure 3).

Flavimycin C (**3**) was isolated as a white solid. It had a molecular formula of $C_{20}H_{22}O_8$ with 10 degrees of unsaturation, as determined by HRESIMS data at m/z 391.1385 (calcd. 391.1387 for $C_{20}H_{23}O_8$, $[M + H]^+$), which was supported by the ^{13}C NMR and DEPT spectral data. The IR spectrum of **3** featured typical absorption bands for hydroxyl (3449 cm^{-1}). The 1H NMR spectrum (Table 1) of **3** exhibited one methyl (δ_H 1.88), one methoxy (δ_H 3.64), one methine (δ_H 4.30), one methylene (δ_H 4.54 d, $J = 15.0\text{ Hz}$; 4.65 d, $J = 15.0\text{ Hz}$), and two hydroxyl protons (δ_H 8.55, δ_H 8.68). The ^{13}C NMR (Table 2) and DEPT spectra displayed 10 well-resolved carbon atom signals, dividing into six quaternary carbons that were assigned to one benzene ring, one methylene (δ_C 65.8), one methine (δ_C 66.1), one methoxy carbon (δ_C 60.2), and one methyl (δ_C 9.5). The NMR data of **3** were very similar to those of **8** except for the absence of the methylene signal, and instead, the presence of the methine signal of C-3 (δ_H 4.30/ δ_C 66.1) in **3**. Combined with molecular formula, **3** was deduced to be a symmetrical dimeric derivative. The above data suggested **3** was a symmetrical dimer of **8**, connecting at C-3/C-10 between the two units (Figure 2), which was further confirmed by the HMBC correlation from H-3 to C-10. Thus, the planar structure of **3** was confirmed as shown (Figure 1), and named flavimycin C. The 1H and ^{13}C NMR spectra (Tables 1 and 2) of this aromatic polyketide dimer only exhibited a set of signals of aromatic polyketide monomer. There were three possible absolute configurations of two chiral carbons C-3 and C-10 in **3**. The obvious negative optical activity ($[\alpha]_D^{20} = -70.0$) and the Cotton effect indicated that compound **3** was not a mesomer, which implied the possibility of 3*R*, 10*S* was excluded. Consequently, the absolute configurations of C-3 and C-10 were the same

(3*S*, 10*S* or 3*R*, 10*R*). The absolute configuration of **3** was understood to be 3*R*, 10*R* by comparing the experimental and simulated ECD curves (Figure 3).

The known compounds: epicocconigrone A (**4**) [24]; 2-(10-formyl-11,13-dihydroxy-12-methoxy-14-methyl)-6,7-dihydroxy-5-methyl-4-benzofurancarboxaldehyde (**5**) [25]; epicoccolide B (**6**) [26]; eleganketal A (**7**) [27]; 1,3-dihydro-5-methoxy-7-methylisobenzofuran (**8**) [28]; and 2,3,4-trihydroxy-6-(hydroxymethyl)-5-methylbenzyl-alcohol (**9**) [29] were identified by comparing their NMR data with those reported in the literature.

The new compounds **1–3** are all aromatic polyketide dimers, particularly compounds **1** and **2** simultaneously featuring consistent 6/6/6/6 heterotetracyclic ring cores and compounds **1–3** co-occurrence in the same marine-derived fungus suggest that they should originate from the same biogenetic pathway. A plausible biosynthetic pathway toward the formation of compounds **1–3** can be proposed by detailed analysis of their structures (Scheme 1).



Scheme 1. Putative biosynthetic pathways toward the formation of compounds **1–3**.

2.2. In Vitro Evaluation of α -Glucosidase Inhibitory Activity

All compounds were tested for their α -glucosidase inhibitory activities using a reported method [30], with acarbose as the positive control. The results revealed that compounds **1**, **4–7**, and **9** showed more potent inhibitory activity (IC_{50} values ranging from 17.04 ± 0.28 to $292.47 \pm 5.87 \mu\text{M}$) than acarbose (IC_{50} , $822.97 \pm 7.10 \mu\text{M}$) (Table 3). The potent α -glucosidase inhibitory activity of epicocconigrone A (**4**) and epicoccolide B (**6**) has been already reported [31]. It could be noted herein that the number of hydroxyl groups of polyhydroxy phenolic compounds was important for α -glucosidase inhibitory activity, as reflected by the low IC_{50} values of compounds **4** and **6**, while structures with fewer hydroxyl groups (compounds **1** and **5**) exhibited little activity.

Table 3. α -Glucosidase inhibitory activities of compounds 1–9.

Compounds	IC ₅₀ ± SD (μM) ^a
1	292.47 ± 5.87
2	–
3	–
4	25.69 ± 0.30
5	40.07 ± 4.64
6	17.04 ± 0.28
7	49.53 ± 2.45
8	–
9	130.63 ± 2.87
Acarbose ^b	822.97 ± 7.10

^a Values represent means ± SD based on three parallel experiments. ^b Positive control.–no activity at a concentration of 200 μM.

3. Materials and Methods

3.1. Fungal Material and Fermentation

The fungal strain *A. insulicola* was isolated from deep-sea sediments, which were collected from the South China Sea at the depth of 2500 m. After grinding, the sample (1.0 g) was diluted to 10^{−2} g/mL with sterile H₂O, 100 μL of which was spread on potato dextrose agar medium (200.0 g potato, 20.0 g glucose, and 20.0 g agar per liter of seawater) plates containing chloramphenicol as a bacterial inhibitor. It was identified by its morphological characteristics and ITS gene sequences (GenBank accession No. ON413861), the used primers of which were ITS1 (TCCGTAGGTGAACCTGCGG) and ITS4 (TCCTCCGCTTATTGATATGC). A reference culture of *A. insulicola* was deposited at the Hainan Provincial Key Laboratory for Functional Components Research and Utilization of Marine Bio-resources, Haikou, China.

3.2. Culture Conditions

The fungal strain *A. insulicola* was cultured in potato dextrose broth medium (consisting of 200.0 g/L potato, 20.0 g/L glucose, and 1000.0 mL deionized water), and incubated on a rotary shaker (150 rpm) for 72 h at 28 °C. Thereafter, 3 mL of seed broth was transferred to fifty 1000 mL Erlenmeyer flasks containing solid rice medium (each flask contained 80 g rice and 120 mL seawater), used for fermentation. The flasks were incubated under static conditions at room temperature for 30 days.

3.3. General Experimental Procedures

Optical rotation was measured using a Modular Circular Polarimeter 5100 polarimeter (Anton Paar, Austria). The NMR spectra were measured on Bruker Avance 500 NMR spectrometer (Bruker, Bremen, Germany) and Bruker DRX-600 spectrometer (Bruker Biospin AG, Fällanden, Germany) using TMS as an internal standard. HRESIMS were determined with an API QSTAR Pulsar mass spectrometer (Bruker, Bremen, Germany). ECD and UV spectra were recorded on a MOS-500 spectrometer (Biologic, France). IR data were measured on a Nicolet 380 infrared spectrometer (Thermo Electron Corporation, Madison, WI, USA). Analytic HPLC was performed with an Agilent Technologies 1260 Infinity II equipped with an Agilent DAD G1315D detector (Agilent, Palo Alto, CA, USA), the separation columns were (COSMOSIL-packed C₁₈, 5 mm, 4.6 mm × 250 mm). Semi-preparative HPLC was performed on reversed-phased columns (COSMOSIL-packed C₁₈, 5 mm, 10 mm × 250 mm). Silica gel (60–80, 200–300 and 300–400 mesh, Qingdao Marine Chemical Co. Ltd., Qingdao, China) and Sephadex LH-20 (Merck, Germany) were used for column chromatography. TLC was conducted on precoated silica gel GF254 plates (Qingdao Marine Chemical Co. Ltd., Qingdao, China), and spots were detected by spraying with 10% H₂SO₄ in EtOH followed by heating.

3.4. Extraction and Isolation

After the fermentation of the strain, the cultures were extracted with EtOAc, then filtered with filter paper. After repeating the procedure three times, the EtOAc extract was evaporated under a reduced pressure to obtain a crude extract (124.0 g). The crude extract was dispersed in water and extracted with petroleum ether, ethyl acetate and *n*-butanol three times, respectively. After vacuum concentration, the petroleum ether extract (11.3 g), ethyl acetate extract (34.0 g) and *n*-butanol extract (20.0 g) were obtained, respectively. Then, the EtOAc extract (34.0 g) was subjected to silica gel vacuum liquid chromatography using step gradient elution with CHCl₃/MeOH (1:0, 200:1, 150:1, 100:1, 80:1, 50:1, 20:1, 10:1, 0:1, *v/v*) to obtain 13 fractions (Fr.1–Fr.13). Fr.4 (425.0 mg) was applied to Sephadex LH-20 gel chromatography eluted with CHCl₃/MeOH (1:1, *v/v*) to give six subfractions (Fr.4.1–Fr.4.6). Fr.4.3 (150.5 mg) was subjected to silica gel column chromatography (petroleum ether/EtOAc, 10:1, *v/v*) to afford nine subfractions (Fr.4.3.1–Fr.4.3.9). Fr.4.3.9 (40.5 mg) was separated by semi-preparative HPLC, eluting with 45% MeOH/H₂O to yield compound 2 (*t*_R 11.5 min, 4.5 mg), and Fr.4.3.7 (29.8 mg) was separated by semi-preparative HPLC, eluting with 35% MeOH/H₂O to give compound 8 (*t*_R 15.3 min, 4.2 mg). Fr.6 (1.15 g) was applied to ODS chromatography eluting with MeOH/H₂O (10%–100%) to give thirteen subfractions (Fr.6.1–Fr.6.13). Fr.6.11 (91.5 mg) was subjected to Sephadex LH-20 (eluted with 100% MeOH) and then purified by semi-preparative HPLC (eluted with 48% MeOH/H₂O) to give compound 1 (*t*_R 21.9 min, 11.1 mg). Fr.6.12 (58.9 mg) was subjected to Sephadex LH-20 (eluted with 100% MeOH) and then purified by semi-preparative HPLC (eluted with 65% MeOH/H₂O) to give compound 5 (*t*_R 10.0 min, 4.2 mg). Fr.6.6 (72.3 mg) was purified on silica gel (petroleum ether/EtOAc, 3:2, *v/v*) to yield compound 3 (7.5 mg). Fr.9 (10.0 g) was subjected to Sephadex LH-20 gel chromatography eluted with MeOH to give ten subfractions (Fr.9.1–Fr.9.10). Fr.9.7 (2.1 g) was subjected to silica gel column chromatography (CH₂Cl₂/MeOH, 100:1, *v/v*), and subsequently purified by semi-preparative HPLC, eluting with 50 % MeOH/H₂O to yield compounds 4 (*t*_R 12.0 min, 5.1 mg) and 6 (*t*_R 18.5 min, 2.7 mg). Fr.9.6 (1.67 g) was separated by Sephadex LH-20 column chromatography eluted with MeOH and then purified by silica gel column chromatography eluting with petroleum ether/EtOAc (3:1; *v/v*) to obtain compound 9 (5.1 mg). Fr.9.8 (0.8 g) was subjected to silica gel column chromatography (CH₂Cl₂/MeOH, 35:1, *v/v*), and subsequently purified by semi-preparative HPLC, eluting with 55 % MeOH/H₂O to yield compound 7 (*t*_R 6.8 min, 8.1 mg).

Epicocconigrone C (1): Yellow film. $[\alpha]_D^{20} = +98.0$ (*c* 0.10, MeOH); UV (MeOH) λ_{\max} (log ϵ): 237 (4.31) nm; 261 (3.91) nm; 309 (4.27) nm; 359 (4.06) nm; IR (KBr) ν_{\max} (cm⁻¹): 3413, 1669, 1466, 1395, 1355, 1296, 1117. ¹H and ¹³C NMR data see Tables 1 and 2; HRESIMS [M + Na]⁺ *m/z* 411.0698 (calcd. for C₁₉H₁₆O₉Na, 411.0687).

Epicocconigrone D (2): Yellow film. $[\alpha]_D^{20} = +57.0$ (*c* 0.10, MeOH); UV (MeOH) λ_{\max} (log ϵ): 234 (4.26) nm; 260 (4.04) nm; 309 (4.21) nm; 365 (4.19) nm; IR (KBr) ν_{\max} (cm⁻¹): 3446, 2931, 1626, 1469, 1359, 1226, 1154, 1115. ¹H and ¹³C NMR data see Tables 1 and 2; HRESIMS [M + Na]⁺ *m/z* 427.1004 (calcd. for C₂₀H₂₀O₉Na, 427.1000).

Flavimycin C (3): White film. $[\alpha]_D^{20} = -70.0$ (*c* 0.10, MeOH); UV (MeOH) λ_{\max} (log ϵ): 232 (4.15) nm; 284 (3.56) nm; IR (KBr) ν_{\max} (cm⁻¹): 3449, 2928, 1606, 1478, 1376, 1264, 1110, 1027. ¹H and ¹³C NMR data see Tables 1 and 2; HRESIMS [M + H]⁺ *m/z* 391.1385 (calcd. for C₂₀H₂₃O₈, 391.1387).

3.5. ECD Calculation

The conformers of compounds were generated using the Confab [32] program ebbed in the Openbabel 3.1.1 software, and further optimized with xtb at GFN2 level [33]. The conformers with population over 1% were subjected to geometry optimization using the Gaussian 16 package [34] at B3LYP/6-31G(d) level and proceeded to calculation of excitation energies, oscillator strength, and rotatory strength at B3LYP/TZVP level in the polarizable continuum model (PCM, methanol). The ECD spectra were Boltzmann-weighted and generated using SpecDis 1.71 software [35].

3.6. α -Glucosidase Inhibitory Activity

All the assays were carried out under 0.1 M sodium phosphate buffer (PH = 6.8). The samples were dissolved with DMSO and diluted into a series of gradient concentrations (final concentrations of 6.25, 12.5, 25, 50, 100, 200, 400, and 800 μ M). The 10 μ L sample was mixed with 100 μ L α -glucosidase solution (0.2 U/mL, Sigma) and shaken well, then added to a 96-well plate and placed at 37 °C for 15 min. Subsequently, 40 μ L of 2.5 mM 4-nitrophenyl- α -D-glucopyranoside was added and further incubated at 37 °C for 15 min. Finally, the OD value of each well was detected at 405 nm wavelength of microplate reader. Acarbose was used as a positive control. The control was prepared by adding DMSO instead of the sample in the same way as the test. The blank was prepared by adding sodium phosphate buffer instead of 4-nitrophenyl- α -D-glucopyranoside using the same method. The percentage inhibition was calculated using the following equation:

$$\% \text{ inhibition} = \frac{(\text{OD}_{\text{control}} - \text{OD}_{\text{sample}})}{(\text{OD}_{\text{control}} - \text{OD}_{\text{blank}})} \times 100$$

4. Conclusions

In summary, two new tetracyclic cores of integrastatins, named epicocconigrone C–D (1–2), one new dimeric isobenzofuran, named flavimycin C (3), and six known compounds (4–9) were isolated from fermentation cultures of the deep-sea sediment-derived fungus *A. insulicola*. The biological evaluation revealed compounds 1, 4–7, 9 exhibited significant α -glucosidase inhibitory with IC_{50} values ranging from 17.04 ± 0.28 to 292.47 ± 5.87 μ M, among which compound 6 was the most potent α -glucosidase inhibitor, with an IC_{50} value 48-fold stronger than positive control acarbose. Comparing the structure of compounds 1, 4, 5 and 6 revealed the α -glucosidase inhibitory activity was greatly enhanced after the hydroxyl group replaced the methoxy group, which further confirmed that polyhydroxy phenolic compounds were efficient α -glucosidase inhibitors, and provided a reference value for the synthesis of novel α -glucosidase inhibitors. In conclusion, the study has enriched the structural diversity of phenolic compounds and provided a promising lead toward the development of novel α -glucosidase inhibitors.

Supplementary Materials: The following supporting information can be downloaded at: <https://www.mdpi.com/article/10.3390/md21030157/s1>, Figures S1–S30: 1D, 2D NMR, MS, UV, and IR spectra of compounds 1–3.

Author Contributions: Conceptualization, Y.Z. and F.L.; methodology, Y.Z. and F.L.; software, Y.Z., F.L. and H.D.; validation, W.Z., Y.Z., W.C., F.L. and H.D.; formal analysis, Y.Z. and H.W.; investigation, W.Z. and W.C.; resources, Y.Z., F.L. and H.D.; data curation, W.Z. and W.C.; writing—original draft preparation, W.Z., Y.Z., H.W. and F.L.; writing—review and editing, Y.Z., F.L., H.W. and H.C.; visualization, W.Z., Y.Z. and F.L.; supervision, Y.Z., F.L. and H.D.; project administration, Y.Z., F.L. and H.D.; funding acquisition, Y.Z. and F.L. All authors have read and agreed to the published version of the manuscript.

Funding: This work was financially supported by Natural Science Foundation of Hainan (322MS131, 220RC702), National Natural Science Foundation of China (41776093), and Financial Fund of the Ministry of Agriculture and Rural Affairs, P. R. China (NFZX2023).

Institutional Review Board Statement: Not applicable.

Informed Consent Statement: Not applicable.

Data Availability Statement: The authors declare that all relevant data supporting the results of this study are available within the article and its Supplementary Materials file, or from the corresponding authors upon request.

Conflicts of Interest: The authors declare no conflict of interest.

References

1. Kashtoh, H.; Baek, K.H. Recent updates on phytoconstituent alpha-glucosidase inhibitors: An approach towards the treatment of type two diabetes. *Plants* **2022**, *11*, 2722. [[CrossRef](#)] [[PubMed](#)]
2. Malik, A.; Ardalani, H.; Anam, S.; McNair, L.M.; Kromphardt, K.J.K.; Frandsen, R.J.N.; Franzyk, H.; Staerk, D.; Kongstad, K.T. Antidiabetic xanthenes with α -glucosidase inhibitory activities from an endophytic *Penicillium canescens*. *Fitoterapia* **2020**, *142*, 104522. [[CrossRef](#)]
3. Du, X.P.; Wang, X.; Yan, X.; Yang, Y.F.; Li, Z.P.; Jiang, Z.D.; Ni, H. Hypoglycaemic effect of all-trans astaxanthin through inhibiting α -glucosidase. *J. Funct. Foods* **2020**, *74*, 104168. [[CrossRef](#)]
4. Jiang, L.L.; Wang, Z.; Wang, X.Y.; Wang, S.J.; Cao, J.; Liu, Y. Exploring the inhibitory mechanism of piceatannol on α -glucosidase relevant to diabetes mellitus. *RSC Adv.* **2020**, *10*, 4529–4537. [[CrossRef](#)] [[PubMed](#)]
5. Attjioui, M.; Ryan, S.; Ristic, A.K.; Higgins, T.; Goni, O.; Gibney, E.; Tierney, J.; O'Connell, S. Kinetics and mechanism of α -glucosidase inhibition by edible brown algae in the management of type 2 diabetes. *P. Nutr. Soc.* **2020**, *79*, E633. [[CrossRef](#)]
6. Fallah, Z.; Tajbakhsh, M.; Alikhani, M.; Larijani, B.; Faramarzi, M.A.; Hamedifar, H.; Mohammadi-Khanapostani, M.; Mahdavi, M. A review on synthesis, mechanism of action, and structure-activity relationships of 1,2,3-triazole-based α -glucosidase inhibitors as promising anti-diabetic agents. *J. Mol. Struct.* **2022**, *1255*, 132469. [[CrossRef](#)]
7. Shah, M.; Bashir, S.; Jaan, S.; Nawaz, H.; Nishan, U.; Abbasi, S.W.; Jamal, S.B.; Khan, A.; Afridi, S.G.; Iqbal, A. Computational analysis of plant-derived terpenes as α -glucosidase inhibitors for the discovery of therapeutic agents against type 2 diabetes mellitus. *S. Afr. J. Bot.* **2021**, *143*, 462–473. [[CrossRef](#)]
8. Zahid, H.F.; Ali, A.; Ranadheera, C.S.; Fang, Z.X.; Dunshea, F.R.; Ajlouni, S. In vitro bioaccessibility of phenolic compounds and alpha-glucosidase inhibition activity in yoghurts enriched with mango peel powder. *Food Biosci.* **2022**, *50*, 102011. [[CrossRef](#)]
9. Abdelli, I.; Benariba, N.; Adjdir, S.; Fekhikher, Z.; Daoud, I.; Terki, M.; Benramdane, H.; Ghalem, S. In silico evaluation of phenolic compounds as inhibitors of A-amylase and A-glucosidase. *J. Biomol. Struct. Dyn.* **2020**, *39*, 816–822. [[CrossRef](#)]
10. Machida, S.; Mukai, S.; Kono, R.; Funato, M.; Saito, H.; Uchiyama, T. Synthesis and comparative structure-activity study of carbohydrate-based phenolic compounds as α -glucosidase inhibitors and antioxidants. *Molecules* **2019**, *24*, 4340. [[CrossRef](#)]
11. Catarino, M.D.; Silva, A.M.S.; Mateus, N.; Cardoso, S.M. Optimization of phlorotannins extraction from *fucus vesiculosus* and evaluation of their potential to prevent metabolic disorders. *Mar. Drugs* **2019**, *17*, 162. [[CrossRef](#)] [[PubMed](#)]
12. Mateos, R.; Pérez-Correa, J.R.; Domínguez, H. Bioactive properties of marine phenolics. *Mar. Drugs* **2020**, *18*, 501. [[CrossRef](#)] [[PubMed](#)]
13. Zhu, Y.X.; Chen, W.Q.; Kong, L.; Zhou, B.X.; Hua, Y.; Han, Y.; Li, J.J.; Ji, J.; Fu, M.; Liu, W.W.; et al. Optimum conditions of ultrasound-assisted extraction and pharmacological activity study for phenolic compounds of the alga *Chondrus ocellatus*. *J. Food Process. Preserv.* **2022**, *46*, E16400. [[CrossRef](#)]
14. Naveen, J.; Baskaran, R.; Baskarana, V. Profiling of bioactives and in vitro evaluation of antioxidant and antidiabetic property of polyphenols of marine algae *Padina tetrastratica*. *Algal Res.* **2021**, *55*, 102250. [[CrossRef](#)]
15. Rengasamy, K.R.R.; Sadeer, N.B.; Zengin, G.; Mahomoodally, M.F.; Cziáky, Z.; Jekó, J.; Diuzheva, A.; Abdallah, H.H.; Kim, D.H. Biopharmaceutical potential, chemical profile and in silico study of the seagrass-*Syringodium isoetifolium* (Asch.) Dandy. *S. Afr. J. Bot.* **2019**, *127*, 167–175. [[CrossRef](#)]
16. Sun, C.X.; Zhang, Z.P.; Ren, Z.L.; Yu, L.; Zhou, H.; Han, Y.X.; Shah, M.; Che, Q.; Zhang, G.J.; Li, D.H.; et al. Antibacterial cyclic tripeptides from Antarctica-sponge-derived fungus *Aspergillus insulicola* HDN151418. *Mar. Drugs* **2020**, *18*, 532. [[CrossRef](#)]
17. Wu, Q.X.; Jin, X.J.; Draskovic, M.; Crews, M.S.; Tenney, K.; Valeriote, F.A.; Yao, X.J.; Crews, P. Unraveling the numerous biosynthetic products of the marine sediment-derived fungus, *Aspergillus insulicola*. *Phytochem. Lett.* **2012**, *5*, 114–117. [[CrossRef](#)]
18. Wu, Q.X.; Crews, M.S.; Draskovic, M.; Sohn, J.; Johnson, T.A.; Tenney, K.; Valerick, F.A.; Yao, X.J.; Bjeldanes, L.F.; Crews, P. Azonazine, a novel dipeptide from a Hawaiian marine sediment-derived fungus, *Aspergillus insulicola*. *Org. Lett.* **2010**, *12*, 4458–4461. [[CrossRef](#)]
19. Sun, C.X.; Liu, X.Y.; Sun, N.; Zhang, X.M.; Shah, M.; Zhang, G.J.; Che, Q.; Zhu, T.J.; Li, J.; Li, D.H. Cytotoxic nitrobenzoyl sesquiterpenoids from an Antarctica sponge-derived *Aspergillus insulicola*. *J. Nat. Prod.* **2022**, *85*, 987–996. [[CrossRef](#)]
20. Zhao, H.Y.; Anbuhezhan, R.; Sun, W.; Shao, C.L.; Zhang, F.L.; Yin, Y.; Yu, Z.S.; Li, Z.Y.; Wang, C.Y. Cytotoxic nitrobenzoyloxy-substituted sesquiterpenes from sponge-derived endozoic fungus *Aspergillus insulicola* MD10-2. *Curr. Pharm. Biotechnol.* **2016**, *17*, 271–274. [[CrossRef](#)]
21. Wang, S.; Zeng, Y.B.; Yin, J.J.; Chang, W.J.; Zhao, X.L.; Mao, Y. Two new azaphilones from the marine-derived fungus *Penicillium sclerotiorum* E23Y-1A. *Phytochem. Lett.* **2022**, *47*, 76–80. [[CrossRef](#)]
22. Wang, Z.; Zeng, Y.B.; Zhao, W.B.; Dai, F.H.; Chang, W.J.; Lv, F. Structures and biological activities of brominated azaphilones produced by *Penicillium sclerotiorum* E23Y-1A. *Phytochem. Lett.* **2022**, *52*, 138–142. [[CrossRef](#)]
23. Zeng, Y.B.; Wang, Z.; Chang, W.J.; Zhao, W.B.; Wang, H.; Chen, H.Q.; Dai, F.H.; Lv, F. New azaphilones from the marine-derived fungus *Penicillium sclerotiorum* E23Y-1A with their anti-inflammatory and antitumor activities. *Mar. Drugs* **2023**, *21*, 75. [[CrossRef](#)]
24. El Amrani, M.; Lai, D.; Debbab, A.; Aly, A.H.; Siems, K.; Seidel, C.; Schneckeburger, M.; Gaigneaux, A.; Diederich, M.; Feger, D.; et al. Protein Kinase and HDAC Inhibitors from the Endophytic Fungus *Epicoccum nigrum*. *J. Nat. Prod.* **2014**, *77*, 49–56. [[CrossRef](#)]
25. Laszlo, V.; Michael, K.; Astrid, M.E.; Luigi, T. 2-Phenyl-benzofuran derivatives, method for the production thereof and their use. D.E. Patent 10,351,315, 2005.

26. Talontsi, F.M.; Dittrich, B.; Schüffler, A.; Sun, H.; Laatsch, H. Epicoccolides: Antimicrobial and antifungal polyketides from an endophytic fungus *Epicoccum* sp. associated with *Theobroma cacao*. *Eur. J. Org. Chem.* **2013**, *2013*, 3174–3180. [[CrossRef](#)]
27. Luan, Y.P.; Wei, H.J.; Zhang, Z.P.; Che, Q.; Liu, Y.K.; Zhu, T.J.; Mándi, A.; Kurtán, T.; Gu, Q.Q.; Li, D.H. Eleganketal A, a highly oxygenated dibenzospiroketal from the marine-derived fungus *Spicaria elegans* KLA03. *J. Nat. Prod.* **2014**, *77*, 1718–1723. [[CrossRef](#)] [[PubMed](#)]
28. Lee, N.H.; Gloer, J.B.; Wicklow, D.T. Isolation of chromanone and isobenzofuran derivatives from a fungicolous isolate of *Epicoccum purpurascens*. *Bull. Korean Chem. Soc.* **2007**, *28*, 877–879. [[CrossRef](#)]
29. Nishihara, Y.; Takase, S.; Tsujii, E.; Hatanaka, H.; Hashimoto, S. New anti-influenza agents, FR198248 and its derivatives. II. Characterization of FR198248, its related compounds and some derivatives. *J. Antibiot.* **2001**, *24*, 297–303. [[CrossRef](#)] [[PubMed](#)]
30. Yang, L.; Yang, Y.L.; Dong, W.H.; Li, W.; Wang, P.; Cao, X.; Yuan, J.Z.; Chen, H.Q.; Mei, W.L.; Dai, H.F. Sesquiterpenoids and 2-(2-phenylethyl) chromones respectively acting as α -glucosidase and tyrosinase inhibitors from agarwood of an *Aquilaria* plant. *J. Enzym. Inhib. Med. CH.* **2019**, *34*, 853–862. [[CrossRef](#)] [[PubMed](#)]
31. Yan, Z.Y.; Huang, C.Y.; Guo, H.X.; Zheng, S.Y.; He, J.R.; Lin, J.; Long, Y.H. Isobenzofuranone monomer and dimer derivatives from the mangrove endophytic fungus *Epicoccum nigrum* SCNU-F0002 possess α -glucosidase inhibitory and antioxidant activity. *Bioorg. Chem.* **2020**, *94*, 103407. [[CrossRef](#)] [[PubMed](#)]
32. O'Boyle, N.M.; Vandermeersch, T.; Flynn, C.J.; Maguire, A.R.; Hutchison, G.R. Confab-systematic generation of diverse low-energy conformers. *J. Cheminform.* **2011**, *3*, 8. [[CrossRef](#)] [[PubMed](#)]
33. Bannwarth, C.; Ehlert, S.; Grimme, S.J. GFN2-xTB an accurate and broadly parametrized self-consistent tight-binding quantum chemical method with multipole electrostatics and density-dependent dispersion contributions. *Chem. Theory Comput.* **2019**, *15*, 1652–1671. [[CrossRef](#)] [[PubMed](#)]
34. Frisch, M.J.; Trucks, G.W.; Schlegel, H.B.; Scuseria, G.E.; Robb, M.A.; Cheeseman, J.R.; Scalmani, G.; Barone, V.; Petersson, G.A.; Nakatsuji, H.; et al. *Gaussian 16, Revision, C.01*; Gaussian, Inc.: Wallingford, CT, USA, 2019.
35. Bruhn, T.; Schaumloffel, A.; Hemberger, Y.; Bringmann, G. SpecDis: Quantifying the comparison of calculated and experimental electronic circular dichroism spectra. *Chirality* **2013**, *25*, 243–249. [[CrossRef](#)] [[PubMed](#)]

Disclaimer/Publisher's Note: The statements, opinions and data contained in all publications are solely those of the individual author(s) and contributor(s) and not of MDPI and/or the editor(s). MDPI and/or the editor(s) disclaim responsibility for any injury to people or property resulting from any ideas, methods, instructions or products referred to in the content.